Thermal denaturation of a native protein via spinodal decomposition in the framework of first-passage-time analysis

Y. S. Djikaev* and Eli Ruckenstein†
Department of Chemical and Biological Engineering, SUNY at Buffalo, Buffalo, New York 14260, USA
(Received 10 March 2008; published 18 July 2008)

In this paper we present a kinetic model for the thermal unfolding of a native protein. Due to a sufficiently large temperature increase or decrease, the rate with which a cluster of native residues within a protein emits residues becomes larger than the rate of absorption of residues from the unfolded part of the protein in the whole range of cluster sizes up to the size of the whole protein. This leads to the unfolding of the protein in a barrierless way, i.e., as spinodal decomposition. Using the formalism of the first passage time analysis [previously applied also to the problem of protein folding via nucleation by the authors, J. Phys. Chem. B **111**, 886 (2007); J. Chem. Phys. **126**, 175103 (2007)], one can determine the temperature dependence of the rates of emission and absorption of residues by the cluster. Knowing these rates as functions of temperature and cluster size, one can find the threshold temperatures of cold and hot barrierless denaturation as well as the unfolding times at temperatures lower and higher, respectively, than those threshold values. For a numerical illustration, the method is applied to the thermal unfolding of a model protein consisting of 2500 residues.

DOI: 10.1103/PhysRevE.78.011909 PACS number(s): 87.14.E−, 87.14.et

I. INTRODUCTION

Most biologically active proteins have a well-defined three-dimensional native structure [1–3]. The stability of this structure constitutes the core of the "protein denaturation" (i.e., unfolding) problem [4,5] whereof many thermodynamic and kinetic aspects remain obscure [4–9]. The unfolding of a protein results in the loss of its biological functionality which may lead to catastrophic consequences for a living organism.

Protein denaturation can be defined as a process (or sequence of processes) whereby the spatial arrangement of the polypeptide chain(s) within the molecule changes from that of the native protein to a more disordered one [4]. This change may alter the secondary, tertiary, or quaternary structure of the protein. Note that what constitutes denaturation is largely dependent upon its cause. Changes in the structure of proteins can be caused by a variety of factors, such as changes in pH of the protein medium [10–13], in its dielectric constant [12,13] or/and in its ionic strength [14,15], protein contact with liquid-vapor or liquid-liquid interfaces [16,17], high pressure [18], heating or cooling [4–9] (thermal denaturation), etc.

In this paper we propose a kinetic model of the thermal mode of protein denaturation. Both experiments and simulations have provided evidence that a native protein, stable at temperature T_0, can unfold upon both cooling and heating [4–9]. When proteins are exposed to increasing or decreasing temperatures, the loss of their biological functionality occurs over a fairly narrow temperature range. Depending upon the protein and the severity of the heating or cooling, the changes may or may not be reversible. Existing theories of unfolding consider water and the amino acid hydrophobicity as crucial factors not only for the correct folding of proteins but also for the maintenance of this structure and for its unfolding [4,19–28].

Protein unfolding (denaturation) is easier understood at high temperatures where it can be at least partly accounted for by a decreased stability of hydrogen bonding between water molecules and between water and protein residues. With increasing temperature, some bonds in a protein molecule are weakened. The first affected are the long range interactions responsible for the stability of the tertiary structure. As these are weakened and broken, the protein becomes more flexible and its (previously) internal groups become more exposed to the solvent. If heating ceases at this stage, the protein is able to refold to the native structure. Upon further heating, some of the hydrogen bonds that stabilize the helical structure begin to break so that the water molecules can interact and form new hydrogen bonds with the amide nitrogen and carbonyl oxygens of peptide bonds.

Thus, as the helical structure is broken, new hydrogen bonding groups and hydrophobic groups are exposed to the solvent and this leads to an increase in the amount of water bound by the protein molecules. This increases the hydrodynamic radius of the molecule causing the viscosity of the solution to increase. The net result will be an attempt by the protein to minimize its free energy by burying as many hydrophobic groups as possible while exposing as many polar groups as possible to the solvent. Although this is analogous to what occurred when the protein initially folded, it now occurs at a much higher temperature. This greatly weakens the short range interactions that initially govern protein folding and the resulting structures are often very different from those of the native protein.

The widespread existence of protein unfolding at low temperatures is surprising, particularly because it is unexpectedly accompanied by a decrease in entropy [28]. It was shown [5] that the cold denaturation is a general phenomenon caused by the very specific and strongly temperature-dependent interactions of the protein nonpolar groups with water. In contrast to expectations, the hydration of these

*idjikaev@eng.buffalo.edu
†Corresponding author. FAX: (716) 645-3822.
feaeliru@acsu.buffalo.edu

 ©2008 The American Physical Society

groups is favorable thermodynamically, i.e., the Gibbs energy of hydration is negative and increases in magnitude as the temperature decreases [5]. As a result, the polypeptide chain, tightly packed in a compact native structure, unfolds at sufficiently low temperatures by exposing internal nonpolar groups to water.

Computer simulations, based either on Monte Carlo (MC) or on molecular dynamics (MD) methods, have been an essential tool for studying both protein folding and protein denaturation. All theoretical treatments of protein unfolding intended to provide information from computer simulations of the process. So far, virtually no analytical description of protein denaturation has been proposed that would be similar to those [23,29–33] for the nucleation mechanism of protein folding [which is believed to be one of the possible pathways for the transition of a protein from the compact "amorphous" configuration (into which an initially unfolded protein quickly transforms) to the native state].

Recently [31–33], we have presented a different, microscopic model for the nucleation mechanism of protein folding whereby, once a critical number of native tertiary contacts is established, the native structure is formed without passing through any detectable intermediates [3,34–36]. The model makes use of a first-passage-time analysis and is based on pairwise "molecular" interactions (i.e., repulsion and attraction), configurational (dihedral angle) potentials in which protein residues are involved, and confining potential which arises because of the finite size of the protein. The protein itself is treated as a random heteropolymer chain consisting of three types of beads—neutral, hydrophobic, and hydrophilic [3,29,32] (with all the bonds and bond angles equal and constant: the model explicitly takes into account the coupling between amino acids, i.e., the polymer connectivity).

In this paper we propose a similar model for the process of protein denaturation occurring, however, in a barrierless way, i.e., as spinodal decomposition. (Previously [37], it was suggested that the collapse of a single polymer chain to a globular shape involves the formation of a "necklace" configuration, as a first stage, via a spinodal process. This paper concerns an opposite process, namely, protein unfolding, which occurs entirely via spinodal decomposition.) We consider a native protein stable at temperature T_0 and examine the temperature dependence of the rates with which it can emit and absorb residues. At T_0 the absorption rate is greater than the emission rate for large enough clusters (of native residues). The unfolding temperature is determined as the temperature at which the emission rate becomes greater than the absorption rate in the whole range of cluster sizes (including the one corresponding to the entire protein). The temperature dependence of the emission and absorption rates is examined by using the formalism of a first-passage-time analysis [31–33] for a series of temperatures.

II. PROTEIN DENATURATION VIA SPINODAL DECOMPOSITION

In our previous work [31–33] on protein folding we considered a protein as a random heteropolymer [38–41] consisting of N connected beads which can be thought of as representing the α-carbons of various amino acids (Fig. 1). For simplicity, let us consider the case where the heteropolymer consists only [31] of hydrophobic (b) and hydrophilic (l) beads sequentially (and randomly) connected to one another by covalent bonds of equal and constant length η with equal and constant angles $\beta_0=105°$ between two neighboring bonds. Assuming that the composition of a cluster of native residues within a protein (which is in a compact, but nonnative state) remains constant and equal to the overall composition of the protein at all times, one can [31] treat protein folding in terms of unary nucleation and characterize the cluster by ν, the total number of residues therein.

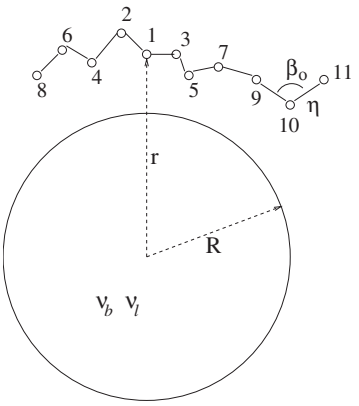

FIG. 1. A piece of a heteropolymer chain around a spherical cluster consisting of $\nu=\nu_b+\nu_l$ beads. Bead 1 is in the plane of the figure, whereas the other beads may all lie in different planes. All bond angles are equal to $\beta_0=105°$ and their lengths are equal to η. The radius of the cluster is R and the distance from the selected bead 1 to the cluster center is r.

As discussed above, the stability of a folded (native) protein can be disrupted by various factors. Continuing the development of a model for the protein folding-unfolding transitions by analogy with the theory of first order phase transitions, one can presume that, depending on the strength of the destabilizing factor(s), the denaturation (unfolding) of the protein can occur either fluctuationally as nucleation (at weak destabilization) or, alternatively, in a barrierless way as spinodal decomposition (at strong destabilization). In the former case (i.e., unfolding via nucleation), the initial unfolding of the protein is thermodynamically unfavorable, but can still occur owing to fluctuations. After the protein unfolds to some critical extent, further denaturation becomes thermodynamically favorable occurring with the decrease in the free energy of the system (protein+medium). In the case of "spinodal decomposition," the protein unfolding is thermodynamically favorable starting from the native state down to full denaturation.

The fundamental kinetic characteristics of the protein unfolding are represented by the rates of emission and absorption of protein residues by a cluster (of native residues). The total rates of emission and absorption of residues by the cluster are given by

$$W^- = W_b^- + W_l^-, \quad W^+ = W_b^+ + W_l^+,$$

where $W_i^- \equiv W_i^-(\nu_b,\nu_l)$ and $W_i^+ \equiv W_i^+(\nu_b,\nu_l)$ $(i=b,l)$ are the rates of emission and absorption, respectively, of beads of

type i by a cluster containing ν_b hydrophobic and ν_l hydrophilic residues. Owing to the chosen approximation [the composition of a cluster of native residues within a protein (which is in a compact but non-native state) remains constant and equal to the overall composition of the protein at all times], the numbers ν_b and ν_l are related to $\nu=\nu_b+\nu_l$ as $\nu_b=x_0\nu$ and $\nu_l=(1-x_0)\nu$, where $x_0=N_b/(N_b+N_l)$ is the mole fraction of hydrophobic residues in the entire protein [$N_i(i=b,l)$ is the total number of residues of type i in the protein]. Thus one can [31] characterize the cluster by ν, the total number of residues therein, and W^+ and W^- can be attributed to a cluster of size ν (with $0\leqslant\nu\leqslant N$),

$$W^w(\nu)=W_b^w(x_0\nu,(1-x_0)\nu)+W_l^w(x_0\nu,(1-x_0)\nu)\equiv W_b^w(\nu_b,\nu_l)+W_l^w(\nu_b,\nu_l)\quad(w=+,-). \tag{1}$$

Being interested in thermal denaturation, let us consider a folded protein at T_0, and assume that it can unfold via spinodal decomposition at either $T>T_u^+>T_0$, which corresponds to hot denaturation, or $T<T_u^-<T_0$, which corresponds to cold denaturation. The corresponding threshold temperatures (T_u^+ and T_u^-, respectively), at which denaturation can occur, can be determined by solving the equation $W^-(N,T)=W^+(N,T)$ with respect to T. If the equation has two solutions, T_u^+ and T_u^-, the protein can unfold upon both heating and cooling. If the equation has just one solution, either T_u^+ or T_u^-, protein denaturation can occur just upon either heating or cooling. In general, $|T_u^+-T_0|$ does not have to be equal to $|T_u^--T_0|$ because denaturation upon heating and cooling is due to several factors, some of which are of different nature in the two cases and even those which are of the same nature may be nonlinear functions of temperature.

The full unfolding time t_u can be evaluated by solving a couple of simultaneous differential equations governing the temporal evolution of the variables ν_b and ν_l for $\nu_b\leqslant N_b$ and $\nu_l\leqslant N_l$,

$$d\nu_i/dt=W_i^+-W_i^-\quad(i=b,l), \tag{2}$$

subject to the initial conditions $\nu_i=N_i$ $(i=b,l)$ at $t=0$ and $\nu_i=0$ $(i=b,l)$ at $t=t_g$. However, by virtue of the chosen approximation $\nu_b/(\nu_b+\nu_l)=\text{const}=x_0$, these simultaneous equations reduce to a single independent equation which [owing to Eq. (1)] can be written in the form

$$\frac{d\nu}{dt}=-[W^-(\nu)-W^+(\nu)] \tag{3}$$

and which has to be solved subject to the initial conditions $\nu=N$ at $t=0$ and $\nu=0$ at $t=t_u$. One can thus obtain

$$t_u\simeq\int_0^N\frac{d\nu}{W^-(\nu)-W^+(\nu)}. \tag{4}$$

The right-hand side (RHS) of this equation is positive because $W^+(\nu)<W^-(\nu)$ in the whole range $0<\nu<N$ at $T=T_u^\pm$ [see Fig. 2(b)]. Note that at $T=T_u^\pm$ the integrand diverges at the upper limit of integration hence care must be taken in applying Eq. (4) at these temperatures (see Sec. II B).

The emission and absorption rates of a cluster (of native residues) of size ν (with $0\leqslant\nu\leqslant N$) are qualitatively presented in Fig. 2(a) (for a protein at temperature $T=T_0$ at which it folds via nucleation), Fig. 2(b) (for a protein at threshold temperatures, $T=T_u^+$ or $T=T_u^-$), and Fig. 2(c) (for a protein at temperature $T>T_u^+$ or $T<T_u^-$ at which it unfolds). As is clear [see Fig. 2(b)], $W^+(\nu)\leqslant W^-(\nu)$ for $\nu\leqslant N$ at temperature $T_u^\pm$ (the equality $W^+=W^-$ holds only for the largest cluster possible, i.e., at $\nu=N$). Therefore if a protein is initially folded at this temperature, it can start unfolding via regular loss of residues from its native structure. The unfolding will occur even faster at $T>T_u^+$ (or $T<T_u^-$), as shown in Fig. 2(c), because in this case $W^+(\nu)<W^-(\nu)$ for all $\nu\leqslant N$ (including $\nu=N$) and the difference $W^-(\nu)-W^+(\nu)$ is greater than for $T=T_u^\pm$ (see Sec. III for more details).

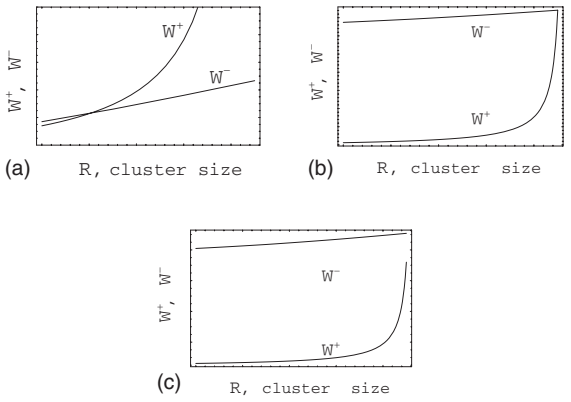

FIG. 2. The qualitative behavior of $W^+(\nu)$ and $W^-(\nu)$, the emission and absorption rates of a cluster (of native residues), as functions of the cluster size R for a protein in the native state (a), for a protein at the threshold temperature of hot or cold denaturation (b), and for a protein at a temperature above the threshold one of hot denaturation or below the threshold one of cold denaturation (c).

A. Determination of $W^+=W^+(\nu)$ and $W^-=W^-(\nu)$ via the first-passage-time analysis

At any given temperature both functions $W^+=W^+(\nu)$ and $W^-=W^-(\nu)$ can be determined by using a first-passage-time analysis [the method was first [42–45] applied to calculating $W^-=W^-(\nu)$ in unary nucleation and later extended [31–33] to both $W^-=W^-(\nu)$ and $W^+=W^+(\nu)$ in protein folding via nucleation]. Let us consider a spherical cluster of native residues (with the structure stabilized by native tertiary contacts) within a protein and denote the distance from its center by r. In our model [31–33] the total potential $\psi_i(r)$ of a selected bead of type i around the cluster contains three terms: the effective pairwise potential $\phi_i(r)$, confining potential ϕ_{cp}, and average dihedral potential $\bar{\phi}_i^\delta(r)$:

$$\psi_i(r)=\phi_i(r)+\bar{\phi}_i^\delta(r)+\phi_{\text{cp}} \tag{5}$$

(for more details see Refs. [31–33]). The first term on the RHS of this equation represents the effective bead-cluster interactions (due to pairwise interactions of the selected residue with those in the cluster). The second term on the RHS of Eq. (5) results from the averaging of the total dihedral angle potential, in which the selected bead is involved, over all the possible configurations of its six nearest neighbors.

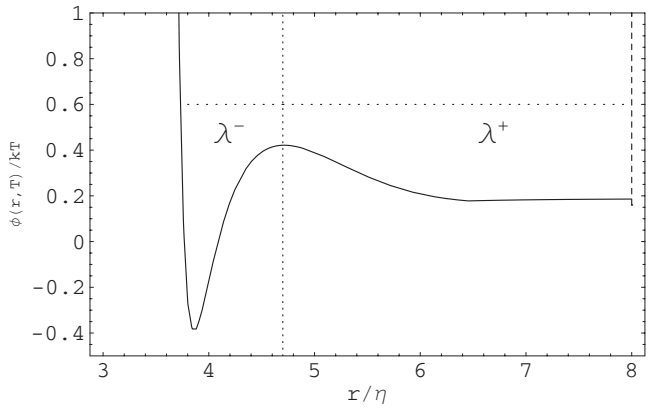

FIG. 3. The total potential field around the cluster of radius $R=3\eta$, which a selected bead (bead 1 in Fig. 1) is subjected to, as a function of the distance r/η from the cluster center. The widths of the inner and outer potential wells are λ^- and λ^+, respectively.

The dihedral angle potential arises due to the rotation of three successive peptide bonds connecting four successive beads and depends not only on the dihedral angle δ (which is an angle between two planes each of which is determined by a sequence of three beads) but also on the nature and sequence of the four beads involved (for more details, see below and Refs. [31–33]). The third term represents the confining potential which arises because all the residues of the protein are linked. Due to these bonds between the residues, none of the latter can be located outside some confining boundary.

It was shown [31–33] that the combination of potentials on the RHS of Eq. (5) gives rise to a double potential well around the cluster with a barrier between the two wells (see Fig. 3). Residues in the inner (closer to the cluster) potential well (i.p.w.) are considered as belonging to the folded cluster, whereas those in the outer potential well (o.p.w.) are treated as belonging to the unfolded part of the protein. Transitions of residues from the inner well into the outer one and vice versa are considered as elementary emission and absorption events, respectively. The double well character of the potential well around the cluster allows one to determine the rates of both emission and absorption of residues by the cluster using a first-passage-time analysis.

Let us consider a heteropolymer bead (i.e., a protein residue) of type i $(i=b,l)$ performing a chaotic motion in a spherically symmetric potential well $\psi(r)$ with one boundary infinitely high (say, at $r=r_a$) and the other one of finite height (say, at $r=r_b$), the mean first passage time τ necessary for the molecule to escape from the well is

$$\tau = \frac{1}{Z}\frac{1}{D}\int_{r_a}^{r_b} dr r^2 e^{-\Psi(r)} \int_{r}^{r_b} dy y^{-2} e^{\Psi(y)} \int_{r_a}^{y} dx x^2 e^{-\Psi(x)} \quad (6)$$

(see the Appendix), where D is the diffusion coefficient of a residue molecule, $\Psi(r)=\psi(r)/k_BT$, and

$$Z = \int_{r_a}^{r_b} dr r^2 e^{-\Psi(r)}. \quad (7)$$

The expression for τ is derived by solving a single-molecule master equation for the probability distribution function of a surface layer molecule (residue/bead) moving in a potential field $\psi(r)$ [46–48,31–33]. The diffusive motion of the bead is assumed to be governed by the Fokker-Planck equation. The Fokker-Planck equation reduces to the Smoluchowski equation (which involves diffusion in an external field) if the relaxation time for the velocity distribution function of the molecule is very short and negligible compared to the characteristic time scale of the passage process (see the Appendix).

The rates of emission and absorption of beads of type i by the cluster (i.e., the numbers of residues of type i escaping from the i.p.w. into the o.p.w. and from the o.p.w. into the i.p.w., respectively, per unit time) are thus provided by

$$W_i^- = \frac{N_i^-}{\tau_i^-}, \quad W_i^+ = \frac{N_i^+}{\tau_i^+}, \quad (8)$$

where N_i^- and N_i^+ denote the numbers of molecules in the i.p.w. and o.p.w., respectively, and τ_i^+ and τ_i^- are the mean first-passage times for the transition of a bead of type i from the o.p.w. into the i.p.w. and from the i.p.w. into the o.p.w., respectively. Applying Eqs. (6) and (7) to calculate W^-, the locations of the boundaries of the i.p.w. must be used, that is, $r_a=R$ and $r_b=R+\lambda^-$, with R the radius of the cluster and λ^- the width of the i.p.w. (Fig. 3). On the other hand, calculating W^+, the locations of the boundaries of the o.p.w. must be used in Eqs. (6) and (7), that is, $r_a=R+\lambda^-+\lambda^+$ and $r_b=R+\lambda^-$, with λ^+ the width of the o.p.w. The quantities N_i^- and N_i^+ can be calculated as the product of the "volume $\times$ number density,"

$$N_i^- = \frac{4\pi}{3}[(R+\lambda^-)^3 - R^3]\rho_f,$$

$$N_i^+ = \frac{4\pi}{3}[(R+\lambda^-+\lambda^+)^3 - (R+\lambda^-)^3]\rho_u,$$

where λ^- and λ^+ are the widths of the inner and outer potential wells, and ρ_f and ρ_u are the number densities of residues in the folded and unfolded parts of the protein.

The term $\bar{\phi}_i^{\delta}(r)$ in $\psi_i(r)$ is due to the r-dependent part of the dihedral angle potential of the whole protein. This is a configurational potential consisting of contributions from every dihedral angle formed by four consecutive beads in the heteropolymer. The potential due to the dihedral angle δ can be modeled, e.g., as [29]

$$\phi_\delta = \epsilon'_\delta(1+\cos\delta) + \epsilon''_\delta(1+\cos 3\delta). \quad (9)$$

Here ϵ'_δ and ϵ''_δ are independent energy parameters which depend on the nature and sequence of the four beads involved in the dihedral angle δ. This potential has three minima, one in the *trans* configuration at $\delta=0$ and two others in the *gauche* configurations at $\delta=\pm\arccos\sqrt{(3\epsilon''_\delta-\epsilon'_\delta)/12\epsilon''_\delta}$ (the former one being the lowest).

Consider a bead 1 (of type b or l) at a distance r from the (center of the) cluster, $r>R$ (see Fig. 1). The total dihedral angle potential $\phi_{i_1}^{\delta}(r)$ of the whole protein chain for a given configuration of beads $1,2,3,\ldots,N$ contains contributions from all the dihedral angles in the heteropolymer each of

which is given by Eq. (9). Clearly, $\phi_{i_1}^{\delta}(r)$ is a function of not only r, but also of coordinates of beads 2 through N, i.e., $\mathbf{r_2}, \mathbf{r_3}, \ldots, \mathbf{r_N}$ [the subscript i_s indicates the type of bead s $(s=1,\ldots,N; i_s=b,l)$]. The contribution to $\phi_{i_1}^{\delta}(r)$ from the dihedral angles involving beads $8,9,\ldots,N$ does not depend on r because those dihedral angles remain unaffected as the position of bead 1 changes because bead 1 participate in the formation of dihedral angles only with three nearest beads on either side of the heteropolymer (beads 2, 4, and 6 on one side and beads 3, 5, and 7 on the other; see Fig. 1). Hence this contribution (const) can be omitted since it can be regarded as affecting only the reference level for $\bar{\phi}_{i_1}^{\delta}(r)$. For a given location of bead 1, various configurations of beads $2,3,\ldots,N$ (subject to the bond length and bond angle constraints as well as to the constraint of excluded cluster volume) lead to various sets of dihedral angles. However, variations in the location of beads $8,9,\ldots,N$ give rise to variations in the dihedral potential which are independent of the position of bead 1, characterized by r. The dihedral term $\bar{\phi}_i^{\delta}(r)$ on the RHS of Eq. (5) can be obtained by averaging $\phi_{i_1}^{\delta}(r)$ with the Boltzmann factor $\exp[-\phi_{i_1}^{\delta 27}(r)/k_BT]$, where $\phi_{i_1}^{\delta 27}(r) \equiv \phi_{i_1}^{\delta 27}(r, \mathbf{r_2}, \ldots, \mathbf{r_7}) = \phi_{i_1}^{\delta}(r) + \Sigma_{s=2}^{7} \phi_{i_s}(\mathbf{r_s})$, over all the possible configurations of beads 2,3,…,7 and assigning the result to the selected bead with fixed coordinates, i.e., to bead 1 (for more details see Refs. [31–33]). Because of this averaging, the average dihedral potential depends on the temperature T, and so does $\psi_i(r)$ in Eq. (5), i.e., $\bar{\phi}_i^{\delta}(r) \equiv \bar{\phi}_i^{\delta}(r,T)$, $\psi_i(r) \equiv \psi_i(r,T)$. Therefore

$$\Psi_i(r) \equiv \Psi_i(r,T) = \psi_i(r,T)/k_BT. \tag{10}$$

It is worthwhile to emphasize that in this model the polymer connectivity is taken into account not only through the confining potential ϕ_{cp}, but also through the average dihedral potential $\bar{\phi}_i^{\delta}(r,T)$. Both of them are constituents of the overall potential field $\psi_i(r,T)$ whereto a selected bead is subjected.

B. The threshold temperatures T_u^- and T_u^+ of cold and hot denaturation and the unfolding times

As is clear, in order to evaluate T_u^+ and/or T_u^-, the minimum and maximum temperatures of hot and cold denaturation, respectively, that occur via spinodal decomposition, it is necessary to know the temperature dependence of the functions $W^-(N)$ and $W^+(N)$, i.e., the functions $W_i^w = W_i^w(\nu,T)$ $(w=+,-; i=b,l)$.

If a protein is subject to both hot and cold denaturation, the corresponding threshold temperatures at which its unfolding can occur via spinodal decomposition (T_u^+ and T_u^-, respectively) can be determined by solving the equation $W^-(N,T) = W^+(N,T)$ with respect to T, i.e.,

$$W^-(N,T_u^+) = W^+(N,T_u^+), \quad W^-(N,T_u^-) = W^+(N,T_u^-) \tag{11}$$

[note that both $W^-(\nu,T)$ and $W^+(\nu,T)$ are monotonic functions of ν]. The first of these equalities means that the threshold temperature of hot denaturation is the lowest temperature at which the emission rate of a cluster is greater than or equal to its absorption rate for clusters of any size, i.e., $W^-(\nu,T) \geqslant W^+(\nu,T)$ for any $\nu \leqslant N$ and $T \geqslant T_u^+$. The second of the equalities in Eq. (11) means that the threshold temperature of cold denaturation is the highest temperature at which the emission rate of a cluster is greater than or equal to its absorption rate for clusters of any size, i.e., $W^-(\nu,T) \geqslant W^+(\nu,T)$ for any $\nu \leqslant N$ and $T \leqslant T_u^-$.

Estimates for the times necessary for the protein to unfold at temperatures $T=T_u^-$ or/and $T=T_u^-$ via spinodal decomposition are given by equations

$$t_u^- \simeq \int_0^{N-0} \frac{d\nu}{W^-(\nu,T_u^-) - W^+(\nu,T_u^-)},$$

$$t_u^+ \simeq \int_0^{N-0} \frac{d\nu}{W^-(\nu,T_u^+) - W^+(\nu,T_u^+)}. \tag{12}$$

Clearly, the unfolding time of hot denaturation at a temperature $T > T_u^+$ is smaller than t_u^+, while the unfolding time of cold denaturation at a temperature $T < T_u^-$ is smaller than t_u^-. The divergence of the integrands at the upper limit of integration at $T=T_u^+$ and $T=T_u^-$ complicates the application of these expressions. The character of the divergence determines whether the t_u's are finite or infinite, but this issue cannot be rigorously addressed unless the ν dependence of $W^-(\nu) - W^+(\nu)$ is explicitly known. Reasonable estimates for t_u^- and t_u^+ can be obtained either by evaluating the integrals at temperatures very close to the threshold ones, $T_u^{\pm}(1 \pm \delta)$ with a positive $\delta \ll 1$, or by slightly decreasing the upper limit of integration (as indicated in Eqs. (12)). The latter method could be substantiated by the effect of fluctuations whereof the physical impact is to decrease the size of the folded cluster of size N but which are not formally included in the model.

The direct application of the method proposed in Refs. [31–33] to determine W_i^w $(w=+,-; i=b,l)$ as functions of ν and T, the temperatures of hot and cold denaturation T_u^+ and T_u^-, and the corresponding unfolding times t_u^+ and t_u^- require lengthy computations. First, the effective pairwise potential $\phi_i(r)$ for a bead of type i in the vicinity of the cluster is constructed as a function of r (distance from the center of a cluster) for a cluster with the numbers of beads therein ν taken on a grid which must be fine enough to be able to accurately construct $\phi_i(r|\nu)$, the effective pairwise potential at fixed r as a function of the continuous variable ν [note that the integration in calculating $\phi_i(r)$ can be carried out analytically if the density ρ inside the cluster is assumed to be uniform]. This function represents the first term on the RHS of Eq. (5) for the potential field around a cluster. It is also needed (see Refs. [32,33]) for calculating the average dihedral potential $\bar{\phi}^{\delta}(r)$ as a function of r for given ν, using the same grid which must be fine enough to construct $\bar{\phi}^{\delta}(r|\nu)$, the average dihedral potential as a function of the continuous variable ν at fixed r. This function represents the second term in on the RHS of Eq. (5) for the potential field around a cluster. Thus one can numerically construct $\psi_i(r,\nu)$, the potential field around a cluster as a function of two variables, r and ν. Knowing this function, one can then calculate the

emission and absorption rates of a cluster (as outlined above or in Refs. [31–33]) as functions of the variable ν for a given T. To determine the temperature dependence of the unfolding times of cold or/and hot denaturation, the emission and absorption rates W_i^+ and W_i^- $(i=b,l)$ must be known as functions of ν for a series of temperature $T \leqslant T_u^-$ or/and $T \geqslant T_u^+$, respectively. Thus it is necessary to carry out the above procedure for a series of temperatures.

III. NUMERICAL CALCULATIONS

To explore the temperature effect on barrierless protein unfolding in the framework of the first-passage-time analysis, we carried out numerical calculations for the unfolding of a large model protein [31] consisting of 2500 hydrophobic and hydrophilic residues, with the mole fraction of hydrophobic residues $\chi_0=0.75$. Hydrophilic residues are readily solvated by water molecules. The presence of water molecules is taken into account implicitly. The formation of hydrogen bonds between water molecules and amino acid residues (particularly hydrophilic ones) has various impacts on the behavior of the polypeptide chain. The pairwise interactions of protein residues are affected by water molecules hydrating them. Dyhedral angle potential may be also affected due to changes in properties of hydrated residues involved. The direct interaction between water molecules hydrogen-bound to protein residues also contributes to residue-residue interactions. All these effects are assumed to be included into the model via the choice of diffusion coefficients and potential parameters of both pairwise and dihedral angle potentials. Pairs of nonadjacent (at least three links apart) beads of type i and j at the distance d from each other were assumed to interact by Lennard-Jones (LJ) potentials $\phi_{ij}(d)=4\epsilon_{ij}[(\eta/d)^{12}-(\eta/d)^6]$ $(i,j=b,l)$, where η is the bond length and ϵ_{ij} $(i,j=b,l)$ is the energy parameter satisfying the mixing rules $\epsilon_{ij}=\sqrt{\epsilon_{ii}\epsilon_{jj}}$. The interactions of nearest and next nearest neighbor beads are completely taken into account by the constant bond length and constant bond angle constraints. The potential due to the dihedral angle δ was modeled according to Eq. (9). The confining potential was considered to be $\phi_{\mathrm{cp}}(r)=0$ for $r<r_{\mathrm{cp}}$ and $\phi_{\mathrm{cp}}(r)=\infty$ for $r \geqslant r_{\mathrm{cp}}$, with the radius of the confining boundary r_{cp} determined by the total number of residues in the protein, densities of residues in its unfolded and folded parts, and the radius of the cluster (folded part): $r_{\mathrm{cp}}=(3/4\pi)^{1/3}[\nu/\rho_f+(N-\nu)/\rho_u]^{1/3}$. A cluster of native residues was characterized by only one independent variable (its radius or total number of residues therein, depending on convenience). This assumption is not essential and served only as a means to simplify the algebra and numerics and to ensure some simplicity of the proposed model.

The numerical values of the parameters involved in the model were chosen as follows. For the potential parameters we have taken $\eta=5.39\times10^{-8}$ cm, $\epsilon_{ll}=(2/700)\epsilon_{bb}$, $\epsilon'_\delta=\epsilon''_\delta=0.3\epsilon_{bb}$, $\epsilon_{bb}=4\times10^{-14}$ erg. The mole fraction of hydrophobic beads was $\chi=0.75$ both in the whole protein and in the cluster. The typical density of the folded protein was evaluated using data from Refs. [49,50] and was set to $\rho_f\eta^3=1.05$, whereas the typical density of the unfolded protein in the compact configuration was set to be $\rho_u=0.25\rho_f$. The temperature dependence of the diffusion coefficients D^{iw} and D^{ow} was modeled as a power law $D_0(1-T_c/T)^\gamma$ as predicted [51] by the mode coupling theory. Taking into account the results of Ref. [52], the diffusion coefficients in the i.p.w. and the o.p.w. were assumed to be related by $D^{\mathrm{iw}}\rho_f=D^{\mathrm{ow}}\rho_u$. Because of the lack of reliable data on the diffusion coefficient of a residue in a native protein, D_0^{iw} was assumed to vary between 10^{-7} cm^2/s and 10^{-9} cm^2/s (much smaller than typical diffusion coefficients for gases but somewhat larger than typical values for solids). At the temperature $T_0=293.15$ K the model protein is predicted [31] to fold into its native state on a time scale of 1–100 s (depending on what numerical value is chosen for the factor D_0^{iw} in the diffusion coefficient D^{iw}). The parameters T_c and γ were chosen to be $T_c=240$ K and $\gamma=2.1$ (for the i.p.w.) and $T_c=245$ K and $\gamma=2.9$ (for the o.p.w.). The parameter T_c determines the temperature at which the "freezing" of the protein residues occurs. Note that the T dependence of D^{iw} arises not only from the direct temperature effect on the chaotic motion of protein residues but also from the indirect effect of either weakening (with increasing T) or strengthening (with decreasing T) their hydrogen bonds with water molecules and between water molecules themselves.

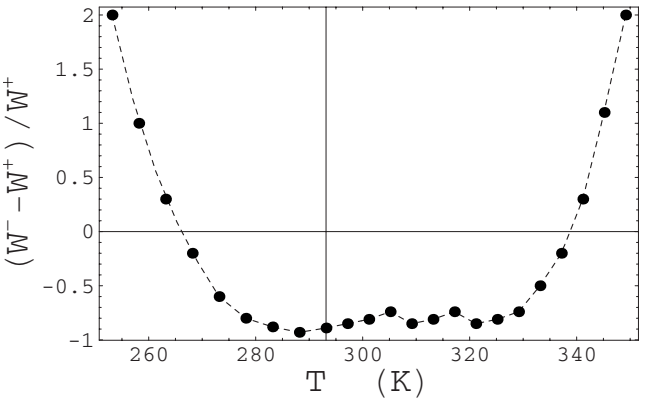

FIG. 4. The function $\omega(T)=[W^-(N,T)-W^+(N,T)]/W^+(N,T)$ plotted vs T for a protein exhibiting both cold and hot denaturation at $T_u^-\simeq247$ K and $T_u^+\simeq338$ K, respectively (for more details, see the text). The dashed line through the points is just for guiding the eye.

The results of numerical calculations are shown in Figs. 4–6. The temperature dependence of the difference between $W^-(N,T)$ and $W^+(N,T)$ is presented in Fig. 4 as a function $\omega(T)\equiv[W^-(N,T)-W^+(N,T)]/W^+(N,T)$ vs T. The threshold temperatures T_u^- and T_u^+ of cold and hot denaturation are determined as the roots of the equation $\omega(T)=0$. For the model protein considered, $T_u^-\simeq267$ K $\simeq T_0-26$ K and $T_u^+\simeq338$ K $\simeq T_0+45$ K. Although denaturation at both low and high temperatures is presumed to be a general property of proteins [53–55], the existence of two roots of the equation $\omega(T)=0$ is not automatic but is possible due to the interplay between the temperature dependence of the diffusion coefficients in the inner and outer potential wells, D^{iw} and D^{iw}. Therefore such a temperature dependence is expected to be most adequate for real proteins exhibiting both cold and hot denaturation. The negative values of this function correspond to con-

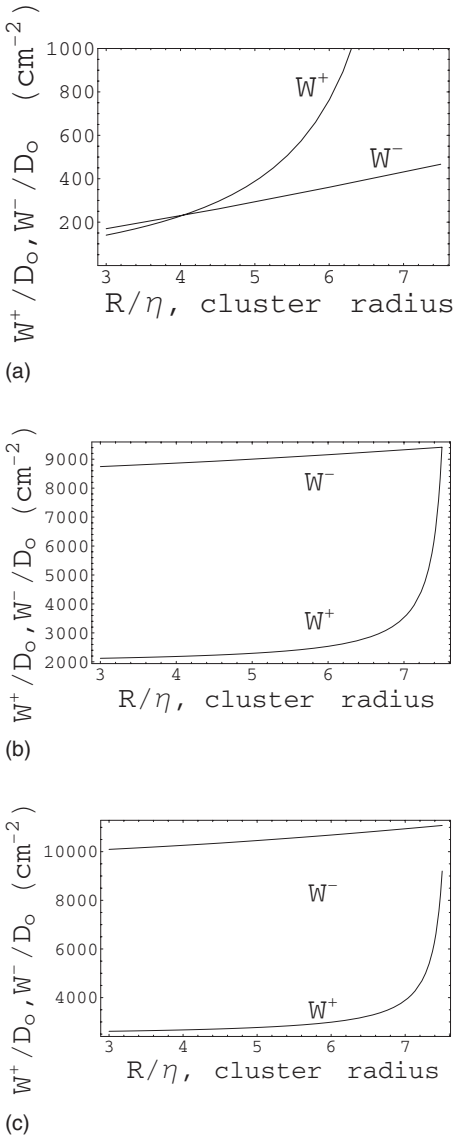

FIG. 5. The emission and absorption rates of a cluster (of native residues), $W^+(\nu)$ and $W^-(\nu)$, as functions of the cluster radius R at $T=T_0=293.15$ K [protein in the native state, (a)], $T=T_u^+\simeq 338$ K [threshold temperature of hot denaturation, (b)], and $T=T_u^+ +5$ K [temperature above the threshold one of hot denaturation, (c)]. The data are presented as $W^{\pm}/D_0$ vs R/η.

ditions when the protein unfolding cannot occur in a barrierless way [see also Fig. 5(a)]. Thus the temperature interval from T_u^- to T_u^+ roughly determines the protein stability range. Clearly, the real stability range may be somewhat narrower because the protein can unfold via nucleation under conditions when the barrierless process is not yet possible (i.e., when T is slightly larger than T_u^- or slightly smaller than T_u^+). The positive values of $\omega(T)$ correspond to conditions under which the protein unfolds in a barrierless way. The larger $\omega(T)>0$, the faster denaturation is expected.

Figure 5 presents $W^+(\nu,T)$ and $W^-(\nu,T)$, the emission and absorption rates of a cluster (of native residues), as functions of ν for three temperatures: $T=T_0$ K [Fig. 5(a)], $T=T_u^+\simeq T_0$ +45 K [Fig. 5(b)], and $T=T_u^+ +10$ K [Fig. 5(c)]. At $T=T_0$ [Fig. 5(a)], $W^+(\nu)<W^-(\nu)$ for $\nu<\nu_c$ and $W^+(\nu)>W^-(\nu)$ for

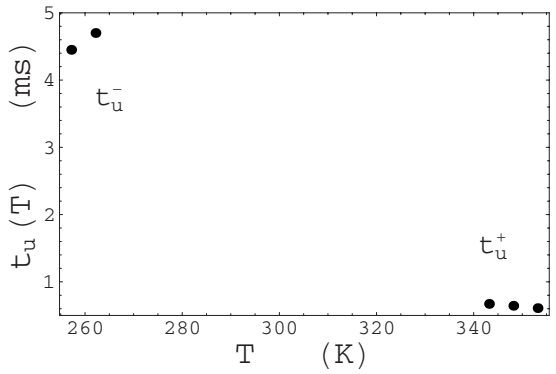

FIG. 6. The temperature dependence of t_u^- (two leftmost points) and t_u^+ (three rightmost points), the time of protein denaturation (via spinodal decomposition) upon cooling and heating, respectively.

$\nu_c<\nu<N$. Clearly, if the protein is initially unfolded at this temperature, it cannot fold via the regular growth of the folded cluster, but it can fold via nucleation. The intersection of $W^+(\nu)$ and $W^-(\nu)$ provides the size ν_c of the critical cluster (nucleus). After the cluster of native residues attains the size ν_c, the whole native structure forms immediately without passing through any detectable intermediate states, because the time t_g of growth of the cluster from size ν_c to size N is much smaller than the time t_ν of formation of the nucleus [18–20]. On the other hand, at temperature T_u^+ [Fig. 5(b)], $W^+(\nu)<W^-(\nu)$ for $0<\nu<N$. Therefore if a protein is initially unfolded at T_u^+, it will never fold, whereas, if it is initially folded at this temperature, it will immediately start unfolding via the loss of residues from its native structure, i.e., in a barrierless way. If the temperature is increased beyond T_u^+ [Fig. 5(c)], the time necessary for the protein to unfold via spinodal decomposition becomes shorter (compared to that time at $T=T_u^+$), because the higher is T above T_u^+ the greater is the positive difference $W^-(\nu)-W^+(\nu)$. Similar behavior is observed when the temperature is decreased down from T_u^-.

Let us denote the times of protein denaturation (via spinodal decomposition) upon heating or cooling at some temperature T by $t_u^+(T)$ and $t_u^-(T)$, respectively. The temperature dependence of the cold denaturation time was calculated at two temperatures below T_u^-, namely, $T=T_u^- -5$ K and $T=T_u^- -10$ K. We have also calculated the time of hot denaturation at three temperatures above T_u^+, namely, $T=T_u^+ +5$ K, $T=T_u^+ +10$ K, and $T=T_u^+ +15$ K. The temperature dependence of t_u^- and t_u^+ is presented in Fig. 6. As expected, the time of barrierless denaturation decreases as T increases above T_u^+ or as T decreases below T_u^-. The unfolding times t_u^- and t_u^+ are inversely proportional to the coefficient D_0 in the temperature dependence of the diffusion coefficient D^{iw}. In Fig. 6, the unfolding times t_u^- and t_u^+ are shown for the case $D_0=10^{-8}$ cm^2/s. Considering D_0^{iw} to be between 10^{-7} cm^2/s and 10^{-9} cm^2/s, the unfolding time of hot denaturation t_u^+ would vary from 0.07 to 7 ms, whereas the unfolding time of cold denaturation t_u^- would vary from 0.5 to 50 ms, consistent with the experimental data on the unfolding times of hot and cold denaturation [53–59]. Many MD simulations report [60,61] much shorter time scales for hot denaturation, but those simulations are usually concerned with the se-

quence of structural changes occurring upon protein unfolding and hence use artificial means to speed up the process and make unfolding occur on a time scale amenable to MD simulations, which is typically less than 100 ns.

IV. CONCLUSIONS

Treating a protein as a heteropolymer with all the bonds having the same constant length and all the bond angles equal and fixed, we recently [31–33] proposed a kinetic model for the nucleation mechanism of protein folding. As a crucial idea of that model, an overall potential around the cluster of native residues wherein a protein residue performs a chaotic motion is considered to be a combination of three terms representing the average dihedral, effective pairwise, and confining potentials. The overall potential as a function of the distance from the cluster center has a double well shape which allows one to determine both the emission and absorption rates of residues by the cluster using the first-passage-time analysis and ultimately evaluate the protein folding time. Note that in this model the polymer connectivity is taken into account through the confining and average dihedral potentials, constituents of the overall potential field in which a selected bead performs a chaotic motion.

In this paper we have presented a similar approach to barrierless protein denaturation (i.e., occurring as spinodal decomposition). The key elements of the approach are the temperature dependent rates with which a cluster of native residues within a compact (but not native) protein emits and absorbs residues. Considering a native protein, stable at temperature $T_0=293.15$ K, we have examined the temperature dependence of the emission and absorption rates of the cluster (which are also functions of the cluster size). This has allowed us to find the threshold temperatures of both hot and cold barrierless denaturation and the time of protein unfolding at various temperatures.

For a numerical illustration of the proposed method, we have considered the thermal denaturation of a model protein [31] which is predicted to fold into its native state at temperature T_0 on a time scale of 1–100 s (depending on what numerical value is chosen for the diffusion coefficient of residues in the folded protein). The model protein considered is a random heteropolymer consisting of a total of 2500 beads of which 75% are hydrophobic and the rest hydrophilic. The purpose of considering such a large protein was to demonstrate the time efficiency of the proposed method. By using the proposed method, the denaturation time of such large proteins can be evaluated much faster than by carrying out direct MD or MC simulations of their unfolding.

We have determined the threshold temperatures of cold and hot denaturation (via spinodal decomposition) of this protein as $T_u^- \simeq 267$ K $\simeq T_0-26$ K and $T_u^+ \simeq 338$ K $\simeq T_0+45$ K, respectively, and examined the temperature dependence of the time of both cold and hot denaturation at temperatures lower and higher than the threshold temperatures of cold and hot denaturation. The unfolding time is inversely proportional to the diffusion coefficient D^{iw} of residues in the native protein for which no reliable data exist in literature. Assuming D^{iw} to vary between 10^{-7} cm^2/s and 10^{-9} cm^2/s, the unfolding time t_u^+ at the threshold temperature of hot denaturation varies from 0.07 to 7 ms, whereas the unfolding time t_u^- at the threshold temperature of cold denaturation varies from 0.5 to 50 ms which is essentially in the range of typical times of protein denaturation. It should be noted that our estimates for $t_u^{\pm}$ are *not* for a general protein, but are for a *particular* protein with the particular size, composition, and interaction parameters as described in the section. Predictions for the unfolding time could differ by orders of magnitude for a different model protein which is quite consistent with the fact that for real proteins unfolding takes place on the time scales that span many orders of magnitude.

APPENDIX: DERIVATION OF EQ. (6) and (7) FOR THE MEAN FIRST-PASSAGE TIME

The mean first-passage-time analysis [42–44] can be used to obtain the rates of emission and absorption of beads by a cluster during protein folding [31–33]. To this end, a bead in the vicinity of the cluster is considered to perform a chaotic motion in the potential wells arising as a combination of the bead-cluster interactions with the dihedral angle potential. The mean first-passage time of a bead escaping from a potential well is calculated on the basis of a kinetic equation governing the chaotic motion of the bead in that potential well. The chaotic motion of the bead is assumed to be governed by the Fokker-Planck equation for the single-particle distribution function with respect to its coordinates and momenta, i.e., in the phase space [46–48]. Prior to the passage event, the evolution of a bead in both the i.p.w. and o.p.w. occurs in a dense enough medium (cluster of folded residues or unfolded, but compact part of the protein), where the relaxation time for its velocity distribution function is very short and negligible compared to the characteristic time scale of the passage process. Under these conditions, the Fokker-Planck equation reduces to the Smoluchowski equation, which involves diffusion in an external field [46,47]. In the case of spherical symmetry it can be written in the form [42–44]

$$\frac{\partial p_i(r,t|r_0)}{\partial t} = D_i r^{-2} \frac{\partial}{\partial r}\left(r^2 e^{-\Psi_i(r)} \frac{\partial}{\partial r} e^{\Psi_i(r)} p_i(r,t|r_0) \right), \quad \text{(A1)}$$

where $p_i(r,t|r_0)$ is the probability of observing a bead of species i $(i=b,l)$ between r and $r+dr$ at time t given that initially it was at a radial distance r_0, D_i is its diffusion coefficient in the well, and $\Psi_i(r)=\psi_i(r)/kT$.

The mean passage time depends on the initial position (distance from the center of the cluster) r_0 of the bead. It is convenient to use the backward Smoluchowski equation [42–44] which expresses the dependence of the transition probability $p_i(r,t|r_0)$ on r_0:

$$\frac{\partial p_i(r,t|r_0)}{\partial t} = D_i r_0^{-2} e^{\Psi_i(r_0)} \frac{\partial}{\partial r_0}\left(r_0^2 e^{-\Psi_i(r_0)} \frac{\partial}{\partial r_0} p_i(r,t|r_0) \right). \quad \text{(A2)}$$

Let us first consider the i.p.w. (with an infinite height boundary at $r_a=R$ and a finite height one at $r_b=R+\lambda^-$) and find the emission rate of beads therefrom. The probability

that a bead i, initially at a distance r_0 within the surface layer, will remain in this region after time t is given by the so-called survival probability [42–44],

$$q_i(t|r_0) = \int_R^{R+\lambda^-} dr r^2 p_i(r,t|r_0) \quad (R < r_0 < R+\lambda^-), \tag{A3}$$

where R is the radius of the cluster and λ_i^- is the width of the potential well determined by the location of the barrier between the i.p.w. and the o.p.w. (see Fig. 2). The probability for the dissociation time to be between 0 and t is equal to $1-q_i(t|r_0)$, and the probability density for the dissociation time is given by $-\partial q_i/\partial t$. The first-passage time is provided by [46–48]

$$\tau_i'(r_0) = -\int_0^\infty t\frac{\partial q_i(t|r_0)}{\partial t}dt = \int_0^\infty q_i(t|r_0)dt. \tag{A4}$$

The equation for the first passage time is obtained by integrating the backward Smoluchowski equation (A2) with respect to r and t over the entire range and using the boundary conditions $q_i(0|r_0)=1$ and $q_i(t|r_0)\to 0$ as $t\to\infty$ for any r_0. This yields [42–44]

$$-D_i r_0^{-2} e^{\Psi(r_0)}\frac{\partial}{\partial r_0}\left(r_0^2 e^{-\Psi_i(r_0)}\frac{\partial}{\partial r_0}\tau_i'(r_0)\right) = 1. \tag{A5}$$

One can solve Eq. (A5) by assuming a reflecting inner boundary of the well ($d\tau_i'/dr_0=0$ at $r_0=R$) and the radiation boundary condition at the outer boundary [$\tau_i'(r_0)=0$ at $r_0=R+\lambda^-$]. One thus obtains for the first-passage time,

$$\tau_i'(r_0) = \frac{1}{D_i}\int_{r_0}^{R+\lambda_i^-} dy y^{-2} e^{\Psi_i(y)}\int_R^y dx x^2 e^{-\Psi_i(x)}. \tag{A6}$$

The average dissociation time τ_i, or the mean first passage time, is obtained by averaging $\tau_i'(r_0)$ with the Boltzmann factor over all possible initial positions r_0:

$$\tau_i = \frac{1}{Z}\int_R^{R+\lambda^-} dr_0 r_0^2 e^{-\Psi_i(r_0)}\tau_i'(r_0) \tag{A7}$$

with

$$Z = \int_R^{R+\lambda^-} dr_0 r_0^2 e^{-\Psi_i(r_0)}. \tag{A8}$$

In a similar fashion, one can determine the mean first-passage time for the transition of a bead from the o.p.w. (with an infinite height boundary at $r_a=R+\lambda^-+\lambda^+$ and a finite height one at $r_b=R+\lambda^-$) into the i.p.w.

[1] C. B. Anfinsen, Science **181**, 223 (1973).
[2] C. Ghelis and J. Yan, *Protein Folding* (Academic, New York, 1982).
[3] T. E. Creighton, *Proteins: Structure and Molecular Properties* (W. H. Freeman, San Francisco, 1984).
[4] W. Kauzmann, Adv. Protein Chem. **14**, 1 (1959).
[5] P. L. Privalov, Crit. Rev. Biochem. Mol. Biol. **25**, 281 (1990).
[6] A. Pastore, S. R. Martin, A. Politou, K. C. Kondapalli, T. Stemmler, and P. A. Temussi, J. Am. Chem. Soc. **129**, 5374 (2007).
[7] M. I. Marqués, Phys. Status Solidi A **203**, 1487 (2006).
[8] O. Gursky and D. Atkinson, Protein Sci. **5**, 1874 (1996).
[9] E. Paci and M. Karplus, Proc. Natl. Acad. Sci. U.S.A. **97**, 6521 (2000).
[10] Z. C. Yang, L. Yang, Y. X. Zhang, H. F. Yu, and W. An, J. Protein Chem. **26**, 303 (2007).
[11] N. Baden and M. Terazima, J. Phys. Chem. B **110**, 15548 (2006).
[12] J. C. Bennett, Methods Enzymol. **11**, 211 (1967).
[13] D. T. Haynie, *Biological Thermodynamics* (Cambridge University Press, Cambridge, England, 2001).
[14] R. Rullera, T. L. Ferreirab, A. H. C. de Oliveirac, and R. J. Ward, Arch. Biochem. Biophys. **411**, 112 (2003).
[15] B. J. Bennion and V. Daggett, Proc. Natl. Acad. Sci. U.S.A. **100**, 5142 (2003).
[16] C. Postel, O. Abillon, and B. Desbat, J. Colloid Interface Sci. **266**, 74 (2003).
[17] N. Michael, A. Brook, and P. Zelisko, Polym. Prepr. (Am. Chem. Soc. Div. Polym. Chem.) **42**, 97 (2001).
[18] Y. Harano and M. Kinoshita, J. Phys.: Condens. Matter **18**, L107 (2006).
[19] W. Kauzmann, Nature (London) **325**, 763 (1983).
[20] C. N. Pace, Biochemistry **40**, 310 (2001).
[21] A. Paliwal, D. Asthagiri, D. P. Bossev, and M. E. Paulaitis, Biophys. J. **87**, 3479 (2004).
[22] D. Paschek and A. E. Garcia, Phys. Rev. Lett. **93**, 238105 (2004).
[23] K. A. Dill, Biochemistry **24**, 1501 (1985); **29**, 7133 (1990).
[24] G. Hummer, S. Garde, A. E. Garcia, and M. E. Paulaitis, Proc. Natl. Acad. Sci. U.S.A. **95**, 1552 (1998).
[25] K. Lum, D. Chandler, and J. D. Weeks, J. Phys. Chem. B **103**, 4570 (1999).
[26] M. Koizumi, H. Hirai, T. Onai, K. Inoue, and M. Hirai, J. Appl. Crystallogr. **40**, 175 (2007).
[27] I. Brovchenko, A. Krukau, N. Smolin, A. Oleinikova, A. Geiger, and R. Winter, J. Chem. Phys. **123**, 224905 (2005).
[28] C-J. Tsai, J. V. Maizel, and R. Nussinov, Crit. Rev. Biochem. Mol. Biol. **37**, 55 (2002).
[29] Z. Guo and D. Thirumalai, Biopolymers **36**, 83 (1995).
[30] J. D. Bryngelson and P. G. Wolynes, Biopolymers **30**, 177 (1990).
[31] Y. S. Djikaev and E. Ruckenstein, J. Phys. Chem. B **111**, 886 (2007).
[32] Y. S. Djikaev and E. Ruckenstein, J. Chem. Phys. **126**, 175103 (2007).
[33] Y. S. Djikaev and E. Ruckenstein, J. Chem. Phys. **128**, 025103 (2008).
[34] J. D. Honeycutt and D. Thirumalai, Proc. Natl. Acad. Sci. U.S.A. **87**, 3526 (1990); Biopolymers **32**, 695 (1992).
[35] V. I. Abkevich, A. M. Gutin, and E. I. Shakhnovich, Biochem-

istry **33**, 10026 (1994).
[36] A. R. Fersht, Proc. Natl. Acad. Sci. U.S.A. **92**, 10869 (1995); Curr. Opin. Struct. Biol. **7**, 3 (1997).
[37] A. Byrne, E. G. Timoshenko, and K. A. Dawson Physica A **243**, 14 (1997); K. A. Dawson, E. G. Timoshenko, and Yu. A. Kuzntesov, *ibid.* **236**, 58 (1997).
[38] E. I. Shakhnovich and A. M. Gutin, J. Phys. A **22**, 1647 (1989).
[39] D. Bratko, A. K. Chakraborty, and E. I. Shakhnovich, J. Chem. Phys. **106**, 1264 (1997).
[40] Z. Konkoli, J. Hertz, and S. Franz, Phys. Rev. E **64**, 051910 (2001).
[41] J. D. Bryngelson and P. G. Wolynes, Proc. Natl. Acad. Sci. U.S.A. **84**, 7524 (1987); J. Phys. Chem. **93**, 6902 (1998).
[42] G. Narsimhan and E. Ruckenstein, J. Colloid Interface Sci. **128**, 549 (1989).
[43] E. Ruckenstein and B. Nowakowski, J. Colloid Interface Sci. **137**, 583 (1990).
[44] B. Nowakowski and E. Ruckenstein, J. Colloid Interface Sci. **139**, 500 (1990).
[45] Y. S. Djikaev and E. Ruckenstein, J. Chem. Phys. **123**, 214503 (2005); **124**, 124521 (2006); **124**, 194709 (2006).
[46] S. Chandrasekhar, Rev. Mod. Phys. **15**, 1 (1943).
[47] C. W. Gardiner, *Handbook of Stochastic Methods* (Springer, New York/Berlin, 1983).
[48] S. Park, M. K. Sener, D. Lu, and K. Schulten, J. Chem. Phys. **119**, 1313 (2003).
[49] Y. Harpaz, M. Gerstein, and C. Chothia, Structure (London) **2**, 641 (1994).
[50] D. M. Huang and D. Chandler, Proc. Natl. Acad. Sci. U.S.A. **15**, 8324 (2000).
[51] A. Mukherjee, S. Bhattacharyya, and B. Bagchi, J. Chem. Phys. **116**, 4577 (2002).
[52] J. O. Hirshfelder, C. F. Curtiss, and R. B. Bird, *Molecular Theory of Gases and Liquids* (Wiley, New York, 1964); W. A. Wakeham, J. Phys. B **6**, 372 (1973).
[53] G. W. Robinson and C. H. Cho, Biophys. J. **77**, 3311 (1999).
[54] B. Ibarra-Molero, G. I. Makhatadze, and J. M. Sanchez-Ruiz, Biochim. Biophys. Acta **1429**, 384 (1999).
[55] H. Georg, C. W. Wharton, and F. Siebert, Laser Chem. **19**, 233 (1999).
[56] U. Mayor, C. M. Johnson, V. Daggett, and A. R. Fersht, Proc. Natl. Acad. Sci. U.S.A. **97**, 13518 (2000).
[57] S. E. Jackson and A. R. Fersht, Biochemistry **30**, 10428 (1991).
[58] S. Spector and D. P. Raleigh, J. Mol. Biol. **293**, 763 (1999).
[59] X. Tang and M. J. Pikal, Pharm. Res. **22**, 1176 (2005).
[60] M. A. Williams, J. M. Thornton, and J. M. Goodfellow, Protein Eng. **10**, 895 (1997).
[61] R. Day and V. Daggett, Proc. Natl. Acad. Sci. U.S.A. **102**, 13445 (2005).